ChemPubSoc Europe

DOI: 10.1002/chem.201402936

CHEMISTRY
A European Journal
Full Paper

Dirhodium Complexes |*Hot Paper*|

Amide-Functionalized Naphthyridines on a Rh^{II}–Rh^{II} Platform: Effect of Steric Crowding, Hemilability, and Hydrogen-Bonding Interactions on the Structural Diversity and Catalytic Activity of Dirhodium(II) Complexes

Mithun Sarkar, Prosenjit Daw, Tapas Ghatak, and Jitendra K. Bera*[a]

Abstract: Ferrocene-amide-functionalized 1,8-naphthyridine (NP) based ligands {[(5,7-dimethyl-1,8-naphthyridin-2-yl)amino]carbonyl}ferrocene (L^1H) and {[(3-phenyl-1,8-naphthyridin-2-yl)amino]carbonyl}ferrocene (L^2H) have been synthesized. Room-temperature treatment of both the ligands with $Rh_2(CH_3COO)_4$ produced $[Rh_2(CH_3COO)_3(L^1)]$ (**1**) and $[Rh_2(CH_3COO)_3(L^2)]$ (**2**) as neutral complexes in which the ligands were deprotonated and bound in a tridentate fashion. The steric effect of the *ortho*-methyl group in L^1H and the inertness of the bridging carboxylate groups prevented the incorporation of the second ligand on the $\{Rh^{II}–Rh^{II}\}$ unit. The use of the more labile $Rh_2(CF_3COO)_4$ salt with L^1H produced a *cis* bis-adduct $[Rh_2(CF_3COO)_4(L^1H)^2]$ (**3**), whereas L^2H resulted in a *trans* bis-adduct $[Rh_2(CF_3COO)_3(L^2)(L^2H)]$ (**4**). Ligand L^1H exhibits chelate binding in **3** and L^2H forms a bridge-chelate mode in **4**. Hydrogen-bonding interactions between the amide hydrogen and carboxylate oxygen atoms play an important role in the formation of these complexes. In the absence of this hydrogen-bonding interaction, both ligands bind axially as evident from the X-ray structure of $[Rh_2(CH_3COO)_2(CH_3CN)_4(L^2H)_2](BF_4)_2$ (**6**). However, the axial ligands reorganize at reflux into a bridge-chelate coordination mode and produce $[Rh_2(CH_3COO)_2(CH_3CN)_2(L^1H)](BF_4)_2$ (**5**) and $[Rh_2(CH_3COO)_2(L^2H)_2](BF_4)_2$ (**7**). Judicious selection of the dirhodium(II) precursors, choice of ligand, and adaptation of the correct reaction conditions affords **7**, which features hemilabile amide side arms that occupy sites *trans* to the Rh–Rh bond. Consequently, this compound exhibits higher catalytic activity for carbene insertion to the C–H bond of substituted indoles by using appropriate diazo compounds, whereas other compounds are far less reactive. Thus, this work demonstrates the utility of steric crowding, hemilability, and hydrogen-bonding functionalities to govern the structure and catalytic efficacyof dirhodium(II,II) compounds.

Introduction

Dirhodium catalysts are widely known for the decomposition of diazo compounds and subsequent carbene transfer to various organic substrates.[1] The majority of the complexes are derived from $Rh_2(CH_3COO)_4$ and retain a paddlewheel geometry around the {Rh–Rh} unit.[1b, 2] Axial and bridging ligands control the stereoelectronic properties,[3] thus influencing the catalytic process.[3b, 4] Strong σ/π-donor ligands at the equatorial sites increase electron density on the rhodium center relative to $Rh_2(CH_3COO)_4$,[5] therefore decreasing the electrophilicity of the metal carbene formed after diazo decomposition and providing a higher level of thermodynamic control of the selectivity.[6] Dirhodium complexes that contain electron-deficient carboxylate groups possess higher Lewis acidity[7] and exhibit enhanced catalytic activity.[8] A series of complexes with various anionic bridging ligands, such as carboxylates,[9] amidinates,[10] triazenides,[11] and orthometalated phosphanes,[12] have been synthesized and their catalytic activities explored. Chiral modification of the bridging ligands has afforded a new class of catalyst for asymmetric synthesis.[1a–d, 2a, 13]

The incorporation of neutral ligands makes the complexes cationic and further increases the electrophilicity of both the metal center and the carbenoid.[14] 1,8-Naphthyridine (NP) and its derivatives have been employed as potential bi-, tri-, and tetradentate ligands (Scheme 1). Kaska and co-workers, with others, have reported several cationic dirhodium complexes with NP, 2-(2-pyridyl)-1,8-naphthyridine (pyNP), and 2,7-bis-(2-pyridyl)-1,8-naphthyridine (bpNP) ligands.[15] The unique *syn*,

[a] *M. Sarkar, P. Daw, T. Ghatak, Prof. J. K. Bera*
Department of Chemistry
Center for Environmental Science and Engineering
Indian Institute of Technology Kanpur, Kanpur 208016 (India)
Fax: (+91) 512-2597436
E-mail: jbera@iitk.ac.in

Supporting information for this article is available on the WWW under http://dx.doi.org/10.1002/chem.201402936.

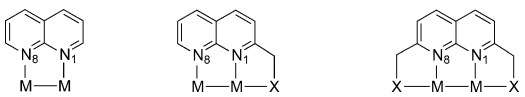

Scheme 1. Different coordination modes of 1,8-naphthyridine-derived ligands

syn-bridging coordination mode of the NP ligands makes them a suitable alternative to bridging carboxylate ligands.[16] The rigid skeleton holds two metal centers in proximity, thus offering synergistic action between the metal centers, and the functionalized side arms provide additional stability by chelation. Although these complexes have long been known, their catalytic utilities have not been evaluated. We proposed to synthesize cationic dirhodium complexes by incorporating suitably designed NP ligands at the equatorial sites and use them as catalysts for a carbene-transfer reaction. Because most of the catalytic reactions of dirhodium complexes occur at the axial sites, these positions need to be accessible for substrate binding. Thus, multidentate naphthyridine ligands with strong axial donors make the complexes catalytically ineffective; however, functionalization of the naphthyridine side arm with an amide group alleviates this problem. The carbonyl oxygen atom binds at the axial site and allows substrate coordination during the catalytic cycle. This type of hemilabile behavior of amide-functionalized naphthyridine has been reported earlier for Pd^{I}–Pd^{I} and Ru^{I}–Ru^{1} platforms by our group.[17]

Herein, we demonstrate the effect of steric crowding, hemilability, and hydrogen-bonding functionalities of L^1H and L^2H ligands to control the structures and catalytic activities of dirhodium(II) compounds (Scheme 2).

Scheme 2. Line drawings of ligands L^1H and L^2H.

Results and Discussion

L^1H and L^2H ligands

Ferrocene-amide-functionalized naphthyridine-based ligands L^1H and L^2H were synthesized by a reaction between 5,7-dimethyl-2-amino-1,8-naphthyridine and 2-amino-3-phenyl-1,8-naphthyridine, respectively, with freshly prepared ferrocenoyl chloride in THF in the presence of Et_3N (Scheme 3). A detailed structural description and spectroscopic data for L^1H has been provided earlier.[18] The ^1H NMR spectrum of L^2H exhibits a characteristic singlet for the amide proton at $\delta = 9.05$ ppm, whereas the amide carbon atom resonates at $\delta = 171.2$ ppm in the

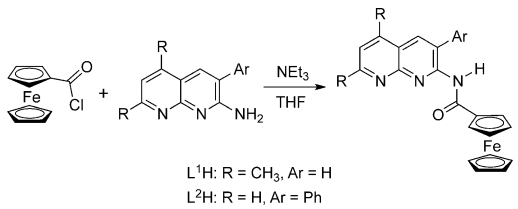

Scheme 3. Synthesis of ligands L^1H and L^2H.

^{13}C NMR spectrum. The IR spectrum shows two strong bands at $\tilde{\nu} = 1678$ and 1662 cm^{-1} for the CO stretching and N–H bending vibrations, respectively. The N–H stretching vibration appears at $\tilde{\nu} = 3449$ cm^{-1}. The ESI-MS spectrum shows a signal at m/z 434.09, which corresponds to the $[M+H]^+$ ion.

The molecular structure of L^2H (Figure 1) reveals that the amide unit is not planar with the naphthyridine ring, as reflected from the dihedral angle N2-C8-N3-C15 $\phi = 58.9(3)^\circ$, as opposed to the near-planar configuration in L^1H.[18] This difference is caused by the substituent phenyl group on the NP ring. The C15–O1 and C15–N3 distances are 1.222(3) and 1.369(3) Å, respectively. The crystal structure of L^2H shows a double hydrogen-bonded dimer that involves an amide hydrogen atom and a proximal nitrogen atom of the naphthyridine unit.

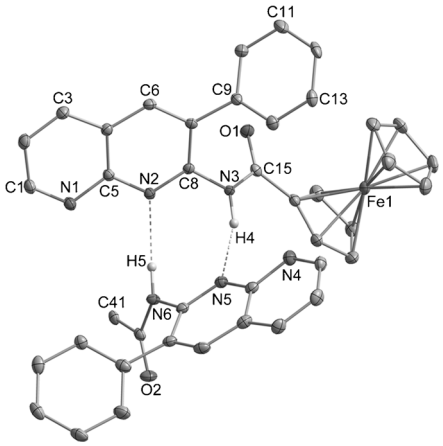

Figure 1. Molecular structure of ligand L^2H, showing intermolecular hydrogen bonding with the important atoms labeled. All the hydrogen atoms, except for N–H, have been omitted for the sake of clarity. The ferrocene rings of the second ligand at C41 have been removed for clarity. Thermal ellipsoids are drawn at the 40% probability level.

Dirhodium complexes

Reaction with $Rh_2(CH_3COO)_4$

Reaction of a solution of L^1H in dichloromethane with $Rh_2(CH_3COO)_4$ at room temperature in a ratio of 1:1 afforded the complex $[Rh_2(CH_3COO)_3(L^1)]$ (**1**) in high yield (80%; Scheme 4). The ligand was deprotonated and only one ligand could be incorporated, even after the use of excess ligand and carrying out the reaction at a higher temperature for a longer time. The absence of the N–H proton in the ^1H NMR spectrum (see Figure S3 in the Supporting Information) indicates deprotonation. Three NP protons appear in the range $\delta = 7.13$–8.02 ppm. Two methyl groups resonate at $\delta = 3.84$ and 2.59 ppm, whereas signals at $\delta = 5.14$, 4.48, and 4.20 ppm in an intensity ratio of 2:2:5 correspond to the cyclopentadienyl (Cp)-ring protons. The ESI-MS spectrum reveals a signal at m/z 767.95 attributed to the $[M+H]^+$ ion. The IR absorption of the amide carbonyl group appears at $\tilde{\nu} = 1635$ cm^{-1}, a difference of 43 cm^{-1} relative to the free ligand.[18]

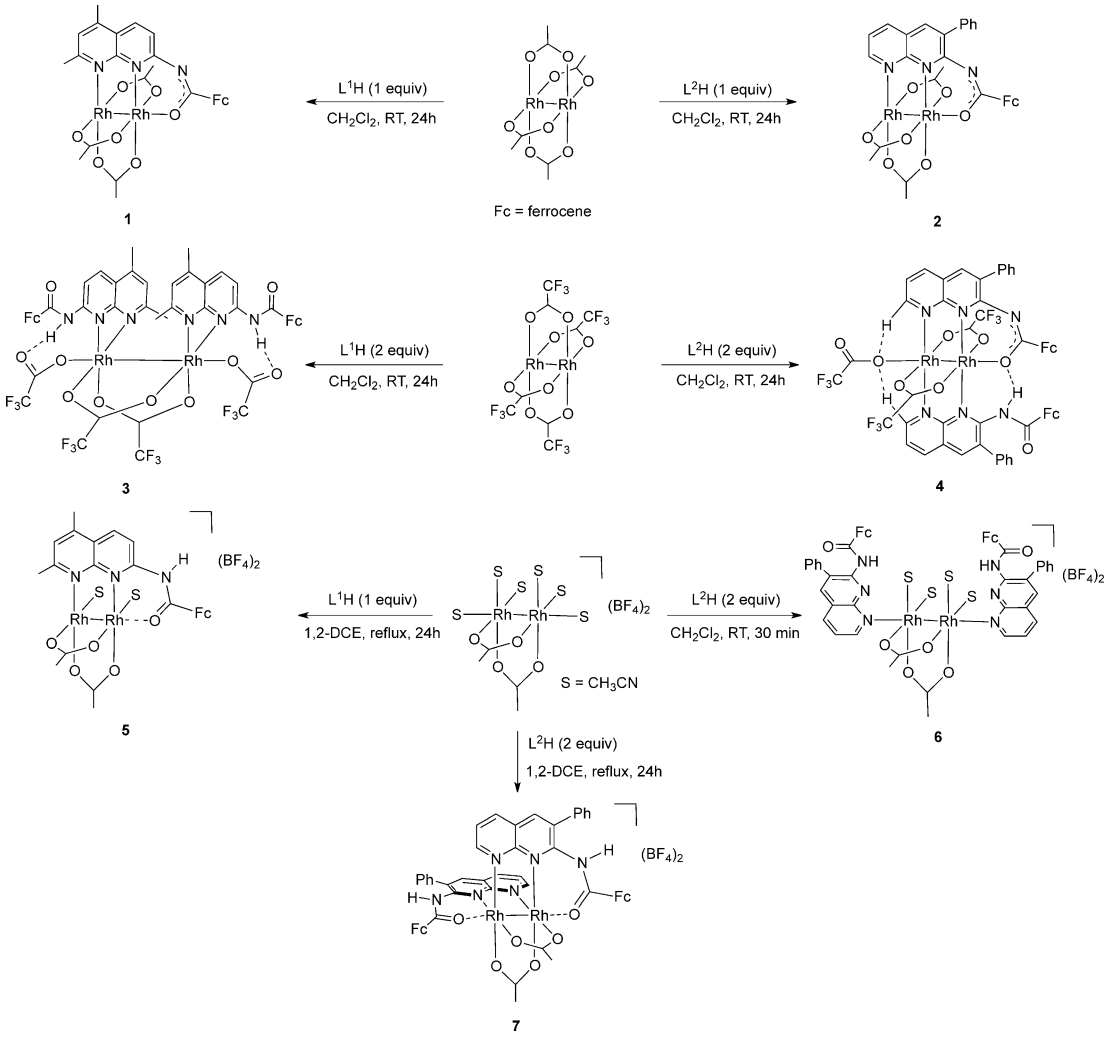

Scheme 4. Syntheses of dirhodium complexes **1**–**7**. 1,2-DCE = 1,2-dichloroethane.

Reaction of $Rh_2(CH_3COO)_4$ with the L^2H ligand under identical reaction conditions produced a red precipitate. The poor solubility of the product in common organic solvents prevented reliable characterization. However, the ESI-MS signal at *m/z* 815.91 (see Figure S9 in the Supporting Information) in acetonitrile suggests the formation of $[Rh_2(CH_3COO)_3(L^2)]$ (**2**), which is analogous to complex **1** (Scheme 4).

The molecular structure of **1** (Figure 2) reveals a paddlewheel structure that consists of three bridging acetate groups and one L^1 ligand, which spans the dimetal unit with deprotonated amide oxygen atoms that occupy one of the axial sites. The second axial site remains blocked by *ortho*-methyl protons (Rh1···H19A/H19C = 2.802(1)/2.798(1) Å). The ^1H NMR spectrum reveals a large downfield shift ($\Delta\delta = 1.12$ ppm) for the *ortho*-methyl protons relative to the free ligand, thus reflecting Rh···H preagostic interactions.[19] The Rh1–Rh2 distance is 2.386(1) Å. The N3–C21 distance (1.329(6) Å) is shorter and the C21–O7 distance (1.271(5) Å) is longer than in L^1H by 0.046 and 0.048 Å, respectively, thus suggesting delocalization of the negative charge throughout the amide skeleton.

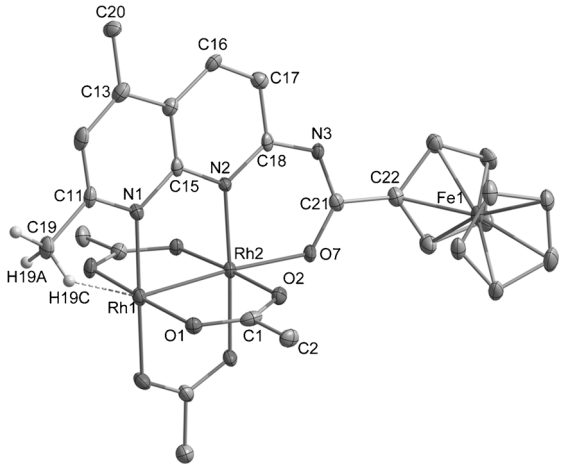

Figure 2. Molecular structure of **1** with the important atoms labeled. All the hydrogen atoms, except for those in the *ortho*-methyl group, have been omitted for the sake of clarity. Thermal ellipsoids are drawn at the 40% probability level.

Reaction with $Rh_2(CF_3COO)_4$

$Rh_2(CF_3COO)_4$, on reaction with L^1H in a ratio of 1:2, gave the adduct $[Rh_2(CF_3COO)_4(L^1H)_2]$ (**3**) as a dark-red solid in 76% yield under identical conditions as for **1** (Scheme 4). The labile trifluoroacetate ions allowed the incorporation of two neutral ligands on the $\{Rh_2\}$ unit. An attempt to isolate a 1:1 adduct by reaction of equimolar amounts of $Rh_2(CF_3COO)_4$ and L^1H only gave **3**, but in decreased yields and starting-material $Rh_2(CF_3COO)_4$ was recovered.

The molecular structure of **3** (Figure 3) shows a four-membered chelate coordination of two L^1H ligands that involve both naphthyridine nitrogen atoms and the Rh centers at

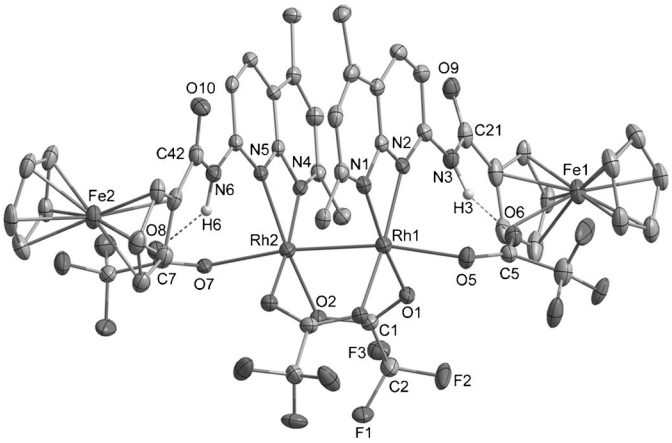

Figure 3. Molecular structure of **3** with the important atoms labeled. All the hydrogen atoms, except for N–H, have been omitted for the sake of clarity. Thermal ellipsoids are drawn at the 40% probability level.

equatorial sites ($\measuredangle$N1-Rh1-N2 and $\measuredangle$N4-Rh2-N5 = 65.0(1)°). Two trifluoroacetate groups bridge the dirhodium unit and the remaining two groups occupy two axial sites. The amide N–H hydrogen atoms engage in hydrogen-bonding interactions with the unbound oxygen atoms of the axial trifluoroacetate groups, therefore stabilizing the rare coordination mode of naphthyridine. Careful examination of the crystal structure reveals that two chelate-bound NP rings are in a *syn*-periplanar conformation around the Rh–Rh bond (the corresponding dihedral angles N1-Rh1-Rh2-N5 and N2-Rh1-Rh2-N4: $\phi = 21.5(1)°$) and are disposed in a head-to-tail fashion. Interestingly, the Rh1–Rh2 distance is quite long, 2.551(1) Å) relative to the other carboxylate-bridged dirhodium complexes in this series.

The singular nature of the ^1H and ^{13}C NMR spectra (see Figure S4 in the Supporting Information) in CD_2Cl_2 suggests a symmetrical structure in solution. The N–H proton appears at $\delta =$ 10.17 ppm in the ^1H NMR spectrum and the amide carbon atom appears at $\delta = 170.2$ ppm in the ^{13}C NMR spectrum. The IR spectrum also shows uncoordinated carbonyl stretching frequencies at $\tilde{\nu} = 1678$ and 1672 cm^{-1}. The ESI-MS spectrum reveals a signal at *m/z* 1314.92, which corresponds to the $[M-CF_3COO]^+$ ion.

The use of L^2H under similar conditions afforded the complex $[Rh_2(CF_3COO)_3(L^2)(L^2H)]$ (**4**; Scheme 4). The molecular structure of **4** comprises of two *trans*-oriented NP ligands, among which one is deprotonated (Figure 4). Two bridging trifluoroacetate moieties and one axially bound trifluoroacetate unit complete the coordination around the $\{Rh_2\}$ unit. Two naphthyridine ligands are arranged in a head-to-head fashion[15g] and are stabilized by a hydrogen-bonding interaction between the N–H group of the neutral L^2H ligand and the axially bound amide oxygen atom of the deprotonated ligand. Similarly, the *ortho*-hydrogen atom of the two naphthyridine ligands engages in a hydrogen-bonding interaction with the axially coordinated trifluoroacetate moiety. The Rh1–Rh2 distance is 2.409(1) Å. The overall structure deviates significantly from a paddlewheel geometry, as indicated from the relevant metrical parameters ($\phi = 18.5(2)$ and 18.1(2)° for N1-Rh1-Rh2-N2 and N4-Rh1-Rh2-N5, respectively).

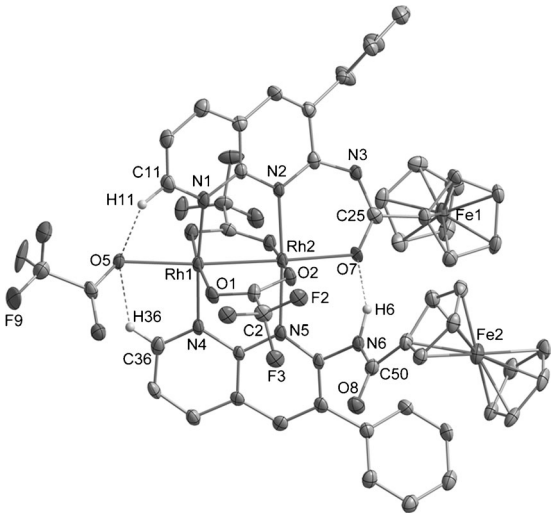

Figure 4. Molecular structure of **4** with the important atoms labeled. All the hydrogen atoms, except for those in the N–H and the *ortho*-NP–H bonds, have been omitted for the sake of clarity. Thermal ellipsoids are drawn at the 40% probability level.

Reaction with $[Rh_2(CH_3COO)_2(CH_3CN)_6](BF_4)_2$

The reaction of equimolar amounts of $[Rh_2(CH_3COO)_2(CH_3CN)_6](BF_4)_2$ and L^1H in 1,2-dichloroethane at reflux produced the bridge-chelate complex $[Rh_2(CH_3COO)_2(L^1H)(CH_3CN)_2(BF_4)_2]$ (**5**) as a red solid within 24 hours (Scheme 4). The use of excess ligand did not lead to the incorporation of the second ligand due to the steric effect of the *ortho*-methyl group at one of the axial sites. The appearance of the N–H proton at $\delta =$ 9.54 ppm and carbonyl carbon atom at $\delta = 174.6$ ppm in the ^1H and ^{13}C NMR spectra, respectively, indicates no deprotonation and weak coordination through the carbonyl oxygen atom to the metal center. A weak IR band at $\tilde{\nu} = 3240$ cm^{-1} (N–H stretching) and strong band at $\tilde{\nu} = 1638$ cm^{-1} (CO stretching) also substantiate this fact.

The molecular structure of **5** was further characterized by X-ray crystallography studies, and the dicationic unit of **5** is shown in Figure 5. This unit consists of two *cis*-bound bridging acetate moieties, two acetonitrile molecules at equatorial sites,

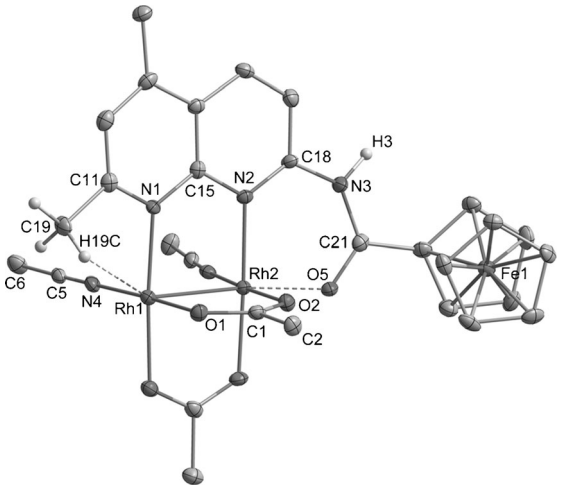

Figure 5. Molecular structure of the dicationic unit $[Rh_2(L^1H)(\mu\text{-}CH_3COO)_2(CH_3CN)_2]$ in **5** with the important atoms labeled. All the hydrogen atoms, except for those in the *ortho*-methyl group and N–H bond, have been omitted for the sake of clarity. Thermal ellipsoids are drawn at the 40% probability level.

and a neutral L^1H ligand that spans the dirhodium unit in a tridentate fashion. The Rh1–Rh2 distance is 2.430(1) Å and N2-C18-N3-C21 dihedral angle is 9.7(1)°, which shows little deviation of the amide plane from the NP ring. The N3–C21 and C21–O5 bond lengths are 1.376(7) and 1.237(7) Å, respectively, which are comparable to the free ligand.

The reaction of L^2H with $[Rh_2(CH_3COO)_2(CH_3CN)_6](BF_4)_2$ in a ratio of 2:1 at room temperature afforded the simple bis-axial adduct $[Rh_2(CH_3COO)_2(L^2H)_2(CH_3CN)_4(BF_4)_2]$ (**6**), which was confirmed by X-ray crystallography studies (Figure 6). The obtained structure shows that both the ligands coordinate to the metal center only through the distal nitrogen atom of naphthyridine, therefore exhibiting similar ^1H and ^{13}C NMR spectra

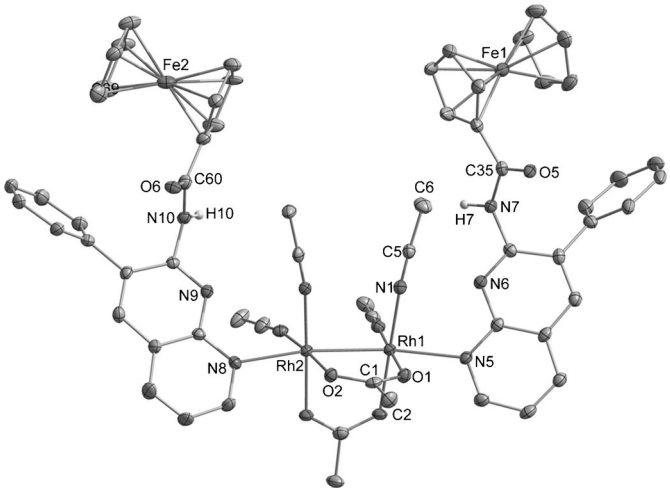

Figure 6. Molecular structure of the dicationic unit $[Rh_2(L^2H)_2(\mu\text{-}CH_3COO)_2(CH_3CN)_4]$ in **6** with the important atoms labeled. All the hydrogen atoms, except for N–H, have been omitted for the sake of clarity. Thermal ellipsoids are drawn at the 40% probability level.

to that of the free ligand. The ESI-MS spectrum exhibits signal at *m/z* 1277, which corresponds to the $[Rh^2(L^2H)_2(BF_4)]^+$ ion.

Instead, when the reaction was carried out at reflux in 1,2-dichloroethane, a bis-bridge chelate complex $[Rh_2(CH_3COO)_2(L^2H)_2(BF_4)_2]$ (**7**) was isolated as a red solid in 73% yield after 24 hours (Scheme 4). The molecular structure of the dicationic unit of **7** (Figure 7) consists of a dirhodium unit spanned by

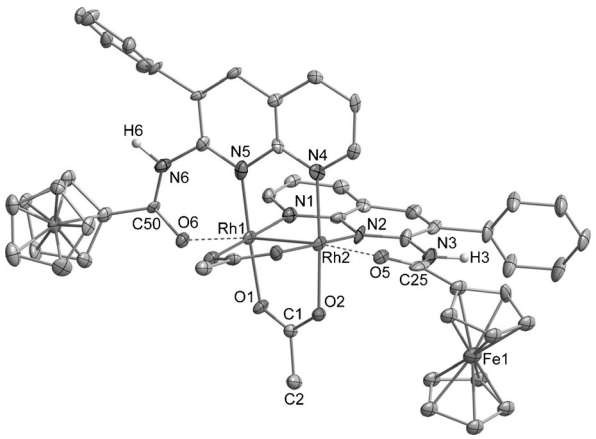

Figure 7. Molecular structure of the cationic unit $[Rh_2(L^2H)]_2(\mu\text{-}CH_3COO)_2]$ in **7** with the important atoms labeled. All the hydrogen atoms, except for N–H, have been omitted for the sake of clarity. Thermal ellipsoids are drawn at the 40% probability level.

two *cis*-L^2H ligands. The N-C-N units of the naphthyridine ligands bridge between two Rh centers, and the sites *trans* to the Rh–Rh bond are occupied by amide oxygen atoms. Thus, two L^2H ligands and two *cis*-bridging acetates complete the coordination around the $\{Rh_2\}$ unit.

The ^1H NMR spectrum of **7** shows two closely separated singlets for N–H protons at $\delta = 9.35$ and 9.34 ppm, whereas the NP, Ph, and Cp protons of two ligands appear in the range 7.60–8.95 ppm (see Figure S7 in the Supporting Information). Interestingly, nine Cp protons of two Cp rings resonate with an intensity ratio of 1:1:1:5:1, unlike other cases in which the Cp protons show intensity ratios of 2:2:5. One of the *ortho*-hydrogen atoms in the substituted ferrocene ring falls in the shielded region of the phenyl ring and appears in the upfield region. The ^{13}C NMR signal at $\delta = 173.8$ ppm and IR stretching frequency at $\tilde{\nu} = 1653\ cm^{-1}$ for the amide carbonyl bond signifies weak coordination to the metal center. The ESI-MS spectrum exhibits at a signal at *m/z* 1277, which is attributed to the $[M-BF_4]^+$ ion.

Effect of steric crowding, lability, and hydrogen-bonding interactions

From the above discussion, it is evident that the formation of complexes **1**–**7** is governed by 1) the steric effect of the *ortho*-methyl group in the L^1H ligand, 2) the basicity/lability of the bridging carboxylate moieties, 3) the structural rigidity of the carboxylate-bridged dirhodium complexes, and 4) hydrogen-bonding interactions between the amide proton and the car-

boxylate oxygen atom. The crystal structures of complexes **1** and **5** show that the *ortho*-methyl group engages the axial site of the $\{Rh_2\}$ core, thus preventing another ligand from approaching. Furthermore, the bridging carboxylate units render a planar structure that involve the $\{Rh_2\}$ unit and NP ring, which is evident from the dihedral angles of $\phi = 1.3(1)$ and $1.1(1)^\circ$ for N1-Rh1-Rh2-N2 in **1** and **5**, respectively. This finding is unlike the Ru^I–Ru^I complex $[Ru_2(L^1H)_2(CO)_4(BF_4)_2]$,[17] in which the NP rings significantly deviate from planarity due to permitted rotation around the Ru–Ru bond (the corresponding angles are $\phi = 33.0(2)$ and $33.6(2)^\circ$ for N1-Ru1-Ru2-N2 and N4-Ru2-Ru1-N5, respectively; Figure 8). Therefore, the *ortho*-methyl groups in the Ru^I–Ru^I complex remain away from the axial sites of the $\{Ru_2\}$ core and allow the incorporation of the second L^1H ligand. This case does not occur for complexes **1** and **5**.

The use of more labile trifluoroacetate moieties allows us to incorporate two ligands into complexes **3** and **4**. The crystal structures reveal the different coordination modes of L^1H and L^2H. Due to the absence of any *ortho*-methyl group in L^2H; two ligands are *trans*-oriented and span the dirhodium core in the most stable bridge-chelate mode in **4**. However, such a *trans* bis-adduct formation is not possible with L^1H in **3** due to steric crowding between the *ortho*-methyl groups. Instead, two ligands bind in a rare bidentate chelate mode and are disposed in a head-to-tail fashion to minimize steric repulsion between them.

Complexes **1**, **2**, and **4** reveal ligand deprotonation in the final structures. Deprotonation under mild conditions in the absence of an external reagent invokes the possibility of hydrogen-bonding interactions between the amide hydrogen and carboxylate oxygen atoms[20] prior to deprotonation. It is assumed that the naphthyridine ligand equilibrates from N8 (distal) to N2 (proximal) coordination to engage in hydrogen-bonding interaction of the amide hydrogen atom with the carboxylate oxygen atom (Scheme 5). This behavior is followed by hydrogen abstraction and subsequent rearrangement from the axial to bridge-chelate coordination. In the absence of hydrogen-bonding interactions, the ligands remain coordinated at the axial sites, which is evident from complex **6**. The bridge-chelate form **7** is obtained only at reflux.

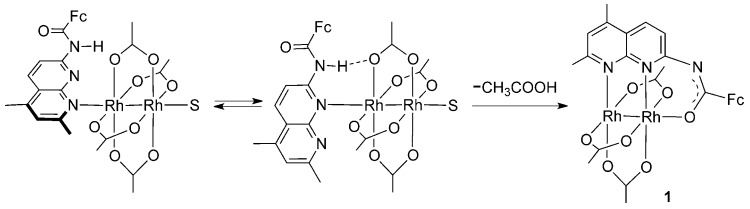

Scheme 5. Hydrogen-bonding-assisted rearrangement of the naphthyridine ligand from axial to bridge-chelate coordination at room temperature.

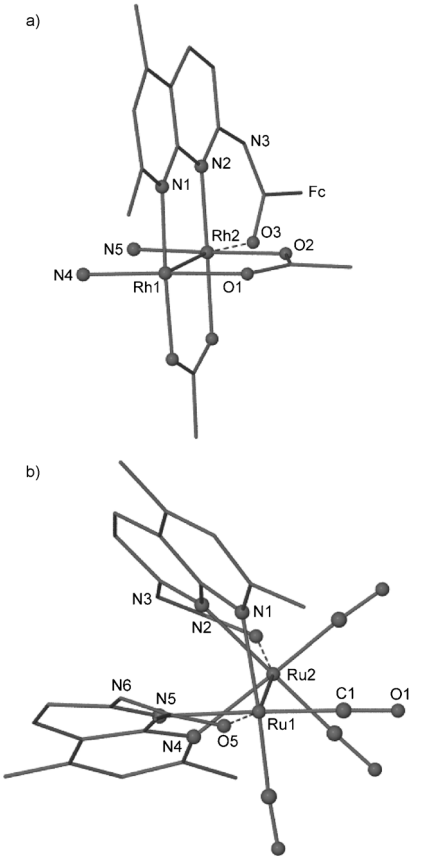

Figure 8. POV-ray diagram of the dicationic unit of a) $[Ru_2(CO)_4(L^1H)_2](BF_4)_2$ (**Ru**^{I}–**Ru**^{I}) and b) $[Rh_2(OAc)_2(L^1H)(CH_3CN)_2](BF4)_2$ (**5**) that shows the deformation of the NP planes. Fc = ferrocene, N4 = N5 = CH_3CN in **5**. Dihedral angles [°]: N1-Ru1-Ru2-N2 = 33.0(2), N4-Ru2-Ru1-N5 = 33.6(2).

Electronic-absorption spectroscopic analysis and electrochemical studies

The electronic-absorption data and electrochemical-potential values for L^1H, L^2H, and **1**–**7** are summarized in Tables 1 and 2, respectively. The ligands exhibit multiple $\pi \rightarrow \pi^*$ transitions between $\lambda = 230$ and 338 nm. Accordingly, the absorptions observed in the UV region for **1**–**7** correspond to ligand-centered $\pi \rightarrow \pi^*$ transitions.[3d,18] The visible regions in the spectra of all the complexes show two intense metal–ligand charge-transfer

Table 1. Electronic-absorption data for L^1H, L^2H, and **1**–**7** in CH_2Cl_2 at room temperature.

Comp.	Absorption data λ_{max} [nm] ($\varepsilon \times 10^{-3}$ [$mol^{-1}dm^3cm^{-1}$])
L^1H	230 (46.5), 327 (16), 336 (15.7), 436 (1.2)
L^2H	231 (54.6), 303 (10.5), 338 (13.5), 484 (1.1)
1	230 (43.5), 314 (19.8), 358 (15.6), 377 (19.5), 436 (6.1), 506 (5.6)
2	230 (51.2), 310 (22.6), 354 (18.3), 376 (21.5), 438 (5.9), 512 (4.8)
3	229 (53.8), 302 (41.5), 332 (34.1), 408 (5.7), 506 (4.5)
4	231 (71.4), 311 (27.2), 351 (20.8), 440 (6.5), 536 (3.6)
5	230 (64.7), 303 (35.7), 341 (29.5), 428 (7.1), 527 (4.7)
6	231 (64.2), 303 (26.8), 341 (20), 440 (3), 516 (2.2)
7	235 (66), 312 (37.3), 336 (24), 349 (22.5), 450 (7.0), 523 (6.4)

Table 2. Electrochemical potentials for L^1H, L^2H, and **1**–**7** in CH_3CN at room temperature.[a]

Compound	Oxidation [V]	Reduction [V]
L^1H	0.64 (76)[b]	−0.84[d], −1.57[d]
L^2H	0.62 (78)[b]	−0.83[d], −1.51[d]
1	0.57[c], 1.24[c], 1.54[c]	−1.02[d], −1.53[d]
2	0.54[c], 1.22[c], 1.58[c]	−1.01[d], −1.42[d]
3	0.72 (66)[b]	−0.57[d], −1.08[d], −1.62[d]
4	0.63 (143)[b]	−0.85[d], −1.30[d], −1.71[d]
5	0.65 (109)[b]	−0.56[d], −1.12[d], −1.57[d]
6	0.58 (75)[b]	−0.57[d], −1.23[d], −1.58[d]
7	0.80 (81)[b]	−0.73[d], −0.95[d], −1.48[d]

[a] Potentials were measured at a Pt disk with Ag/AgCl as the reference electrode, Pt wire as an auxiliary electrode, and 0.1 M $TBAPF_6$ as the supporting electrolyte at a scan rate of 100 mV s^{-1}. [b] Half-wave potentials evaluated from cyclic voltammetry as $E_{1/2}=(E_{p,a}+E_{p,c})/2$; peak potential differences [mV] are given in parentheses. [c] Peak potentials $E_{p,a}$ for irreversible oxidation processes. [d] Peak potentials $E_{p,c}$ for irreversible reduction processes.

(MLCT) bands assigned to $\{Rh_2\}(\pi^*)\rightarrow NP(\pi^*)$.[3d,15i] The higher intensities of the MLCT bands overshadow the much weaker d–d transitions for the ferrocenyl unit[21] and the metal-centered $\{Rh_2\}(\pi^*)\rightarrow\{Rh_2\}(\sigma^*)$ transitions observed in the parent dirhodium complexes.[3d,15b,22]

The electrochemical studies of both ligands show one reversible ferrocenyl oxidation at around +0.6 V and two irreversible reductions at around $E_{p,c}=-0.8$ and −1.5 V. In contrast, only one reduction process is observed for NP, pyNP, and bpNP ligands (at −1.88, −1.68, and −1.56 V, respectively).[3d,15i] Although complexes **1** and **2** show multiple oxidations, complexes **3**–**7** show multiple reductions in their respective cyclic voltammograms. All the complexes show ferrocene-based oxidation below +0.81 V, whereas two additional oxidations occur above +1.2 V for complexes **1** and **2**. These processes are considered to be rhodium centered.[15b] Complexes **1** and **2** exhibit two irreversible reduction processes, whereas an additional reduction below −0.86 V is observed for complexes **3**–**7**. These reductions at lower potentials are attributed to be metal centered.[15b] The occurrence of additional oxidation and reduction processes for complexes **1**, **2**, and **3**–**7** can be explained on the basis of their ligand compositions. The NP ligands in **1** and **2** are anionic, which increases the electron density at the Rh center, thus favoring the oxidation of $Rh_2^{4+}\rightarrow Rh_2^{5+}\rightarrow Rh_2^{6+}$.[23,15b] Complexes **3**–**7** are either cationic and contain neutral NP ligands or consist of more electron-withdrawing trifluoroacetate groups. Therefore, in addition to two ligand-centered reductions, a metal-centered $Rh_2^{4+}\rightarrow Rh_2^{3+}$ reduction is also accessible within the potential range.[15b,24]

Catalytic C–H functionalization of indoles

The transition-metal-catalyzed decomposition of diazo compounds provides one of the most powerful approaches to the functionalization of C–H bonds.[1d,25] Because indole derivatives are important structural motifs in many naturally occurring alkaloids and pharmaceutically active compounds,[26] efforts have been made to functionalize the C3 or C2 positions of substituted indoles selectively by applying this strategy.[27] Wenkert et al. first reported the C3 functionalization of *N*-methylindole with ethyl diazoacetate with Cu bronze as a catalyst, and ethyl 2-(1-methyl-1*H*-indol-3-yl)acetate was obtained in 27% yield.[28] A recent report on the same procedure provided *tert*-butyl 2-(1-methyl-1*H*-indol-3-yl)acetate in 11% yield by using *tert*-butyl diazoacetate as the carbenoid source and a CuO/SiO_2 mixture as the catalyst.[29] Although these catalyst systems and the acceptor carbenoid showed disappointed results, a major breakthrough occurred by using the donor/acceptor diazo compound as the carbenoid source with various dirhodium carboxylate derivatives as catalysts.[30] Muthusamy et al. reported the regiospecific intermolecular C–H insertion of 3-diazooxindoles with various substituted indoles in the presence of $Rh_2(OAc)_4$ in high yield (up to 99%).[31] Fox and co-workers demonstrated the enantioselective C–H functionalization of indoles with ethyl α-alkyl-α-diazoacetates with 0.5 mol% Rh_2(*S*-NTTL)$_4$ (NTTL = *N*-(1,8-naphthaloyl)-*tert*-leucinate) and [Rh_2(*S*-PTTL)$_3$TPA (PTTL = *N*-phthaloyl-*tert*-leucinate, TPA = triphenylacetate) in 82–96% yield with 79–99% enantioselectivity.[9c,32] Lian and Davies developed the enantioselective C–H functionalization of indoles by using vinylcarbenoids in the presence of a catalytic amount (2 mol%) of Rh_2(*S*-biTISP)$_2$ (TISP = 5,5′-(1,3-phenylene)bis[1-(2,4,6-triisopropylphenylsulfonyl)pyrrolidine-2-carboxylate] in 64–86% yield with 86–95% enantioselectivity.[33] Several other metal catalysts, including copper,[34] ruthenium,[35] and iron,[36] have also been used toward this goal. The metal carbenoids flanked by electron-withdrawing and electron-donating groups exhibit greater stability and selectivity over the traditional acceptor rhodium carbenoids (e.g., ethyl diazoacetate), in which the carbene carbon atom lacks donor-group stabilization, and are therefore highly reactive.[14] Furthermore, by incorporating various donor functionalities into the diazo compound, it is possible to obtain a wide range of functionalized products with a particular dirhodium catalyst.

On this backdrop, and with well-characterized dirhodium complexes in hand, we performed a C–H functionalization of indoles. Comparative catalytic studies were carried out for all complexes **1**–**7** and $Rh_2(OAc)_4$ by using three types of carbenoid source, namely, an acceptor (ethyl diazoacetate), a donor/acceptor (methyl phenyldiazoacetate), and an acceptor/acceptor (dimethyl diazomalonate). We rationalized that complex **7** would be the best choice among **1**–7 because it has hemilabile amide groups at both the axial sites, whereas the axial sites in other complexes are less accessible due to strong axial coordination of the ligands (see below). Accordingly, 1-methyl-1*H*-indole, ethyl diazoacetate (acceptor), and $Rh_2(OAc)_4$ underwent a reaction in a ratio of 1:1.2:0.05 in 1,2-dichloroethane at room temperature with one equivalent of dodecane as an internal standard. The reaction was monitored by using GC-MS, and a maximum yield of 56% was obtained within 24 hours (Figure 9). A longer reaction time did not increase the product formation. Next, complex **7** was employed under identical conditions, and only 22% product was obtained, even after 36 hours. Subsequently, the reaction was carried out at higher temperature (60 °C), and we observed 58% product formation

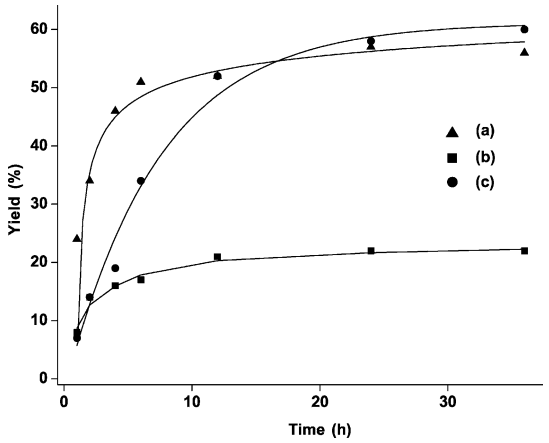

Figure 9. Time- and temperature-dependence curve for C–H functionalization of 1-methyl-1*H*-indole with ethyl diazoacetate and 5 mol% dirhodium catalyst. a) $Rh_2(OAc)_4$ at room temperature, b) complex **7** at room temperature, and c) complex **7** at 60 °C.

within 24 hours (Figure 9). A longer reaction time (36 h) and carrying the reaction out at reflux (85 °C) only led to a marginal increase in the yield (60%), whereas $Rh_2(OAc)_4$ lead to a lower yield due to catalyst decomposition at this temperature.

Lowering the catalyst loading from 5 to 2 mol% did not affect the product formation by much for both $Rh_2(OAc)_4$ and **7**, but further lowering the catalyst loading to 1 mol% gave much lower yields (Table 3). Subsequently, complexes **1**–**6** were tested with 2 mol% of the complexes at 60 °C for 24 hours. Although complex **5** resulted in 45% yield, far less conversion was obtained for complexes **1**–**4** and **6** (Table 3).

Methyl phenyldiazoacetate (donor/acceptor) was used next and the reaction was carried out for *N*-methylindole with 1 mol% $Rh_2(OAc)_4$ and complex **7** independently (the results are summarized in Table 4). At room temperature, 90% yield of methyl 2-(1-methyl-1*H*-indol-3-yl)-2-phenylacetate was isolated within 12 hours for $Rh_2(OAc)_4$, whereas complex **7** produced a marginally increased yield (92%) under identical conditions.

Table 3. Optimization of the reaction conditions and catalysts.[a]

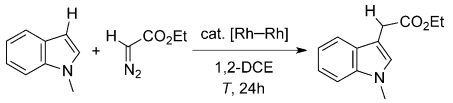

Entry	Catalyst	[mol%]	*T* [°C]	Yield [%][b]
1	$Rh_2(OAc)_4$	5	RT	56
2	$Rh_2(OAc)_4$	2	RT	54
3	$Rh_2(OAc)_4$	1	RT	42
4	**7**	5	60	58
5	**7**	2	60	56
6	**7**	1	60	38
7	**7**	2	85	60
8	**1**	2	60	10
9	**2**	2	60	14
10	**3**	2	60	16
11	**4**	2	60	6
12	**5**	2	60	45
13	**6**	2	60	11

[a] Conditions: Catalyst = 1–5 mol%, 1-methyl-1*H*-indole (1 mmol), slow addition of ethyl diazoacetate (1.2 mmol) over 30 min, and stirring at the respective temperatures for 24 h in a nitrogen atmosphere. [b] The reaction was monitored by using GC-MS and the yield was calculated by using dodecane (1 mmol) as an internal standard.

Table 4. Optimization of the reaction conditions and catalysts.[a]

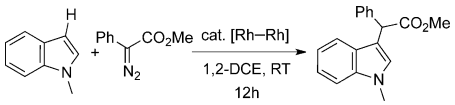

Entry	Catalyst	[mol%]	Yield [%][b]
1	$Rh_2(OAc)_4$	1	90
2	$Rh_2(OAc)_4$	0.5	76
3	**7**	1	92
4	**7**	0.5	72
5	**1**	1	22
6	**2**	1	16
7	**3**	1	35
8	**4**	1	18
9	**5**	1	78
10	**6**	1	55

[a] Conditions: Catalyst = 0.5–1 mol%), 1-methyl-1*H*-indole (1 mmol), slow addition of methyl phenyldiazoacetate (1.2 mmol) over 30 min, and stirring at room temperature for 12 h in a nitrogen atmosphere. [b] Yield of the isolated product.

As in the previous case, a decreased catalyst loading and the use of other dirhodium complexes **1**–**6** produced much lower yields (Table 4). Finally, dimethyl diazomalonate (acceptor/acceptor) was used as the carbenoid source. Although it was readily decomposed by $Rh_2(OAc)_4$ at room temperature,[37] no decomposition of the diazo compound occurred by complex **7** even at refluxing temperature.

With the optimized reaction conditions in hand, the substrate scope of both reactions was examined with complex **7** as the catalyst (the results are summarized in Tables 5 and 6). Substitution at the benzene ring had a less prominent effect as the corresponding products **8b**–**8e** and **9b**–**9e** were isolated in yields of 52–56 and 88–92%, respectively; however, substitution at the C2 position of the pyrrole ring produced a slightly lower yield of **8f** and **9f**. In contrast, substitution of the N–H bond showed a more prominent effect. The unprotected indole produced a mixture of C–H, N–H, and both C–H and N–H insertion products, among which the C–H insertion product **8g** was isolated in 38% yield as the major product and by-products were detected by GC-MS. *N*-acetyl substitution makes the pyrrole ring electron deficient, which therefore remained unreactive toward C–H functionalization for both the diazo compounds. Allyl substitution at N–H showed preferential C–H insertion over cyclopropanation (**8i** and **9h**). Both the reactions were very specific for C3 functionalization, and no isomeric C2 functionalized products were detected. Attempts to obtain the C2-functionalized product by blocking the C2 position only resulted in recovery of the starting material. The use of *N*-methyl-7-azaindole instead of *N*-methylindole remained unsuccessful for ethyl diazoacetate (**8k**), but a moderate yield

Table 5. C–H functionalization of indoles with ethyl diazoacetate.[a]

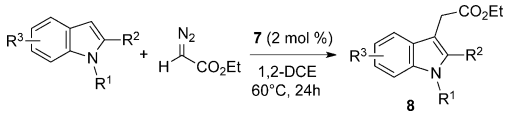

8

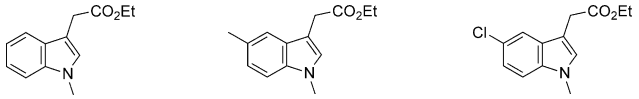

8a, 54%

8b, 56%

8c, 54%

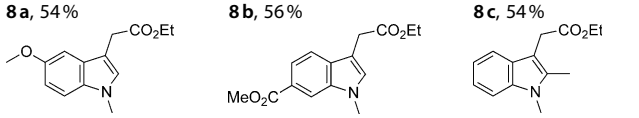

8d, 55%

8e, 52%

8f, 48%

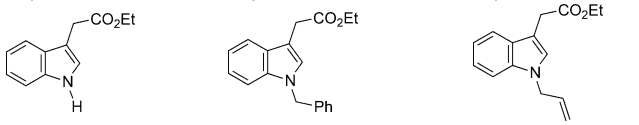

8g, 38%[b]

8h, 50%

8i, 50%

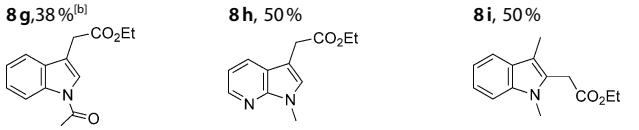

8j, n.r.

8k, n.r.

8l, n.r.

[a] Substituted indole (1 mmol), catalyst **7** (0.02 mmol), slow addition of ethyl diazoacetate (1.2 mmol) over 30 min, and stirring at 60 °C for 24 h in a nitrogen atmosphere. Yield of the isolated product is given. [b] C–H insertion product only. [c] n.r. = No reaction.

Table 6. C–H functionalization of indoles with methyl phenyldiazoacetate[a]

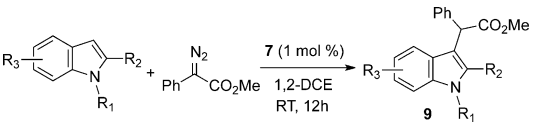

9

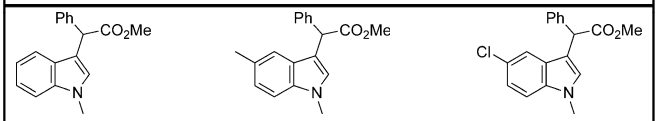

9a, 92%

9b, 90%

9a, 88%

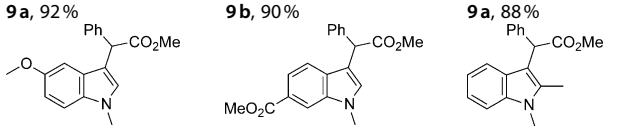

9d, 92%

9e, 90%

9f, 80%

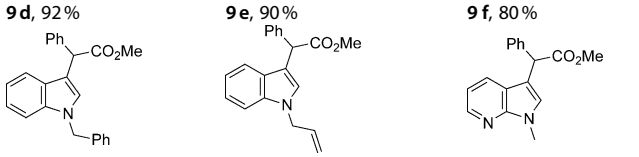

9g, 84%

9h, 86%

9i, 58%

[a] Substituted indole (1 mmol), catalyst **7** (0.01 mmol), slow addition of methyl phenyldiazoacetate (1.2 mmol) over 30 min, and stirring at room temperature for 12 h in a nitrogen atmosphere. Yield of the isolated product is given.

(58%) of the corresponding C–H functionalized product (**9i**) was obtained for methyl phenyldiazoacetate.

All the results obtained above can be explained by comparing the structures of the dirhodium complexes, the nucleophilicity of the diazo compounds, and the formation pathways of the electrophilic metal carbenoids (Scheme 6). Nakamura and

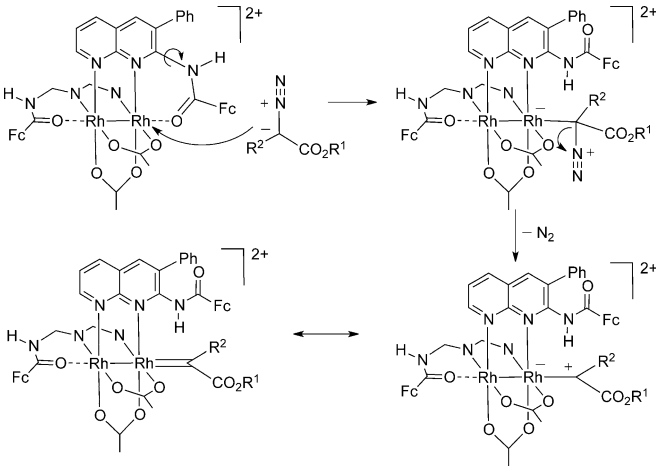

Scheme 6. Decomposition of the diazo compound and the formation of dirhodium carbenoid by complex **7**.

Berry suggested that the reaction occurs only at one axial site while the second metal center acts as an electron sink by forming a 3c/4e bonding manifold that involves two rhodium centers and lone carbene carbon center.[38, 3a] Among all the complexes, $Rh_2(OAc)_4$, **5**, and **7**, with at least one accessible axial site, show much a higher reactivity relative to the other complexes, in which both axial sites are blocked either due to a stronger coordination of neutral/anionic donor ligands or by axial preagostic interactions between the {Rh–Rh} unit and the *ortho*-methyl hydrogen atoms. The lower reactivity of **2** is attributed to its poor solubility in the chlorinated solvent. In the case of **5** and **7**, both the axial sites in the latter are protected by the hemilabile amide groups and offer greater accessibility of the axial sites over **5**, which has only one accessible site. Consequently, **7** shows a much higher reactivity than **5** because the formation of the metal carbenoid involves an initial nucleophilic attack of the diazo compound on the Rh center at the axial site (Scheme 6). Methyl phenyldiazoacetate, with a greater nucleophilic character, forces an outward rotation of the amide group, even at room temperature, to de-coordinate from the axial site, thus allowing the reaction to take place. However, carrying out the reaction at reflux is necessary for ethyl diazoacetate. Dimethyl diazomalonate, with the least nucleophilic character, remained unreactive toward the metal-carbene formation, even at reflux. Thus, catalyst **7** exhibits better selectivity of the diazo compounds than $Rh_2(OAc)_4$ at room temperature, although the reactivities are comparable; furthermore, **7** has a higher thermal stability over $Rh_2(OAc)_4$. Therefore, catalyst 7 has the potential to perform a selective C–H functionalization reaction by carefully choosing the diazo compound and controlling the reaction temperature.

Conclusion

Ferrocene-amide-functionalized 1,8-naphthyridine (NP) based ligands L^1H and L^2H have been synthesized to exploit their hemilabile amide side arm as a weakly coordinating axial ligand on the Rh^{II}–Rh^{II} platform. Depending on the *ortho* substituent, the lability of the bridging carboxylate moieties, and hydrogen-bonding interactions between the amide hydrogen and carboxylate oxygen atoms, a host of structurally diverse compounds have been isolated that vary in the number, nature (neutral/anionic), and coordinating modes of the incorporated ligands. Among all the complexes reported in this study, complex **7**, with two hemilabile amide side arms at the axial sites of the $\{Rh_2\}$ core, shows superior activity toward the C–H functionalization of indoles with appropriate diazo compounds. Although the reactivity of **7** is marginally better than $Rh_2(OAc)_4$, it has a higher thermal stability and exhibits better selectivity toward the diazo compounds at a controlled reaction temperature. Thus, hemilabile ligands appear to serve as a way to improve thermal stability, control the reaction rate, and induce selectivity in the dirhodium catalyst.

Experimental Section

2-Aminonicotinaldehyde,[15i] 2-amino-3-phenyl-1,8-naphthyridine,[39] substituted indoles, dimethyl diazomalonate, and methyl phenyldiazoacetate were prepared by following reported procedures.[29,34–36] Ethyl diazoacetate was purchased from Sigma Aldrich. Dirhodium precursors, such as $[Rh_2(CH_3COO)_4(CH_3CN)_2]$,[40] $[Rh_2(CF_3COO)_4(Et_2O)_2]$,[40] and $[Rh_2(CH_3COO)_2(CH_3CN)_6](BF_4)_2$[41] were prepared as reported earlier.

Syntheses

{[(5,7-Dimethyl-1,8-naphthyridin-2-yl)amino]carbonyl}ferrocene (L^1H): Oxalyl chloride (1.1 mL, 13 mmol) was added dropwise to a suspension of ferrocenecarboxylic acid (2 g, 8.694 mmol) in dichloromethane (50 mL) at 0 °C. A few drops of DMF were added to the reaction mixture, and the reaction began immediately. The mixture was slowly brought to room temperature and stirred for 12 h. All the solvent and excess oxalyl chloride were removed under reduced pressure to afford ferrocenoyl chloride as a dark-red solid in almost quantitative yield. This crude product was directly used in the next step without further purification.

2-Amino-5,7-dimethyl-1,8-naphthyridine (1.66 g, 9.563 mmol) was dissolved in THF (100 mL) and triethylamine (3 mL, 21.6 mmol) was added to the solution. The solution was chilled to 0 °C and a suspension of ferrocenoyl chloride (prepared in the previous step) in THF was added portionwise over 30 min. The resulting mixture was slowly brought to room temperature while a white precipitate of triethylamine hydrochloride deposited on the walls of the flask. Stirring was continued for 12 h at room temperature and then heated to reflux for an additional 12 h. After completion of the reaction, the solvent was removed by means of rotary evaporation. The residue was taken in dichloromethane and extracted with a saturated aqueous solution of sodium bicarbonate. The organic phase was dried over anhydrous Na_2SO_4 and evaporated to obtain a dark-brown solid. The residue was purified by column chromatography on silica gel with ethyl acetate/petroleum ether (1:1) as the eluent to obtain the product as an orange solid (3 g, 90%). ^1H NMR (500 MHz, $CDCl_3$): $\delta = 8.85$ (br s, 1H; NH), 8.57 (d, $J = 8.6$ Hz, 1H; NP), 8.33 (d, $J = 8.9$ Hz, 1H; NP), 7.12 (s, 1H; NP), 4.90 (s, 2H; Cp), 4.49 (s, 2H; Cp), 4.26 (s, 5H; Cp), 2.72 (s, 3H; Me), 2.66 ppm (s, 3H; Me); ^{13}C NMR (126 MHz, $CDCl_3$): $\delta = 170.2$ (NHCO), 162.9 (NP), 154.4 (NP), 153.3 (NP), 145.7 (NP), 135.8 (NP), 122.3 (NP), 118.6 (NP), 113.9 (NP), 74.8 (Cp), 71.8 (Cp), 70.2 (Cp), 68.8 (Cp), 25.4 (Me), 18.2 ppm (Me); IR (KBr): $\tilde{\nu} = 3474$ (br, w, N–H), 3228 (br, w), 3084 (sh, w), 1678 (vs; CO), 1601 (vs; N–H), 1510 (s), 1454 (m), 1404 (m), 1315 (s), 1285 cm^{-1} (s); MS (ESI; CH_3CN): *m/z* 386.0951 $[M+H]^+$.

{[(3-Phenyl-1,8-naphthyridin-2-yl)amino]carbonyl}ferrocene (L^2H): Ligand L^2H was synthesized by following a similar procedure described for the synthesis of L^1H by the reaction between ferrocenecarboxylic acid (2 g, 8.694 mmol) and 2-amino-3-phenyl-1,8-naphthyridine (2.12 g, 9.563 mmol) to obtain an orange solid (2.8 g, 74%). Orange block-shaped crystals of X-ray quality were grown by layering petroleum ether onto a solution of the ligand in ethyl acetate. ^1H NMR (500 MHz, $CDCl_3$): $\delta = 9.05$ (br s, 1H; NH), 8.39 (br s, 1H; NP), 8.16 (br s, 1H; NP), 8.10 (br s, 1H; NP), 7.58 (br s, 1H; NP), 7.52–7.55 (m, 3H; Ph), 7.45–7.48 (m, 2H; Ph), 4.62 (s, 2H; Cp), 4.37 (s, 2H; Cp), 4.11 ppm (s, 5H; Cp); ^{13}C NMR (126 MHz, $CDCl_3$): $\delta = 171.2$ (NHCO), 168.8 (NP), 162.9 (NP), 154.1 (NP), 147.6 (NP), 139.6 (NP), 138.0 (NP), 136.9 (NP), 130.0 (Ph), 129.1 (Ph), 128.4 (Ph), 121.4 (NP), 71.4 (Cp), 70.0 (Cp), 68.9 ppm (Cp); IR (KBr): $\tilde{\nu} =$ 3449 (br, w; N–H), 3195 (br, w), 3080 (sh, w), 1678 (vs; CO), 1662 (vs; N–H), 1608 (m), 1595 (m), 1558 (m), 1522 (m), 1500 (m), 1471 (m), 1457 (m), 1432 (m), 1419 cm^{-1} (m); MS (ESI; CH_3CN): *m/z* 434.0956 $[M+H]^+$.

$[Rh_2(L^1)(\mu\text{-}CH_3COO)_3]$ (1): $Rh_2(CH_3COO)_4$ (40 mg, 0.091 mmol) was added in one portion to (5,7-dimethyl-1,8-naphthyridin-2-yl)aminocarbonylferrocene (L^1H; 40 mg, 0.104 mmol) dissolved in dichloromethane (10 mL). The resulting red solution was stirred at room temperature for 24 h in a nitrogen atmosphere. The solution was concentrated to a small volume under reduced pressure, and diethyl ether/petroleum ether (10 mL, 1:2) was added while stirring to obtain a red precipitate. The precipitate was further washed with petroleum ether (3×10 mL) and dried under vacuum to afford **1** as a red microcrystalline solid (58 mg, 80%). Block-shaped crystals of X-ray quality were grown by layering petroleum ether onto a solution of **1** in dichloromethane in a vacuum-sealed glass tube (o.d. = 8 mm). ^1H NMR (400 MHz, CD_3CN): $\delta = 8.02$ (d, $J =$ 9.2 Hz, 1H; NP), 7.16 (s, 1H; NP), 7.13 (d, $J = 9.6$ Hz, 1H; NP), 5.14 (s, 2H; Cp), 4.48 (s, 2H; Cp), 4.20 (s, 5H; Cp), 3.84 (s, 3H; Me_{NP}), 2.59 (s, 3H; Me_{NP}), 2.10 (s, 3H; Me_{OAc}), 1.60 ppm (s, 6H; Me_{OAc}); ^{13}C NMR (100 MHz, CD_3CN): $\delta = 189.9$ (CO_{OAc}), 185.3 (CO_{OAc}), 172.1 (NP), 166.1 (CO_{NCO}), 163.8 (NP), 158.6 (NP), 148.0 (NP), 143.0 (NP), 134.0 (NP), 125,7 (NP), 121.9 (NP), 71.0 (Cp), 70.7 (Cp), 69.8 (Cp), 69.3 (Cp), 24.3 (Me_{NP}), 22.9 (Me_{OAc}), 22.7 (Me_{OAc}), 17.6 ppm (Me_{NP}); IR (KBr): $\tilde{\nu} = 3098$ (w), 3059 (w), 2988 (w), 2924 (w), 1635 (s, CO_{NCO}), 1593 (vs; OAc), 1572 (vs; OAc), 1433 cm^{-1} (vs); MS (ESI; CH_3CN), *m/z*: 767.95 $[M+H]^+$; elemental analysis (%) calcd for $C_{27}H_{27}N_3O_7Fe_1Rh_2$: C 42.27, H 3.55, N 5.48; found: C 42.78, H 3.64, N 5.22.

$[Rh_2(L^2)(\mu\text{-}CH_3COO)_3]$ (2): Complex **2** was synthesized by following the similar procedure described for the synthesis of complex **1** by reaction of $Rh_2(CH_3COO)_4$ (40 mg, 0.091 mmol) and L^2H (45 mg, 0.104 mmol) to obtain 57 mg (74%) of the product. IR (KBr): $\tilde{\nu} =$ 3094 (w), 3060 (w), 2980 (w), 2924 (w), 1630 (s; CO_{NCO}), 1588 (vs; OAc), 1574 (vs; OAc), 1416 cm^{-1} (s); MS (ESI; CH_3CN): *m/z* 815.9095 $[M+H]^+$; elemental analysis (%) calcd for $C_{31}H_{27}N_3O_7Fe_1Rh_2$: C 45.67, H 3.34, N 5.15; found: C 44.80, H 3.62, N 5.32.

$[Rh_2(L^1H)_2(CF_3COO)_4]$ (3): $Rh_2(CF_3COO)_4$ (50 mg, 0.076 mmol) was dissolved in dichloromethane (10 mL) and L^1H (60 mg, 0.156 mmol) was added in one portion. Immediately after the addition, the

color of the solution became deep red. The solution was further stirred for 24 h at room temperature in a nitrogen atmosphere and then concentrated to a small volume under reduced pressure. Petroleum ether (10 mL) was added to the residue while stirring to obtain a red precipitate, which was further washed with petroleum ether (3×10 mL) and dried under vacuum to afford **3** as a deep-red solid (82 mg, 76%). Block-shaped crystals of X-ray quality were grown by layering petroleum ether onto a solution of **3** in dichloromethane inside a vacuum-sealed glass tube (o.d.=8 mm). ^{1}H NMR (500 MHz, CD_2Cl_2): δ=10.17 (s, 2H; NH), 7.80 (d, J=9.2 Hz, 2H; NP), 7.74 (d, J=9.5 Hz, 2H; NP),6.84 (s, 2H; NP), 4.97 (s, 4H; Cp), 4.61 (s, 4H; Cp), 4.30 (s, 10H; Cp), 2.48 (s, 6H; Me_{NP}), 2.11 ppm (s, 6H; Me_{NP}); ^{13}C NMR (126 MHz, CD_2Cl_2): δ=176.5 (OTfAc), 173.6 (OTfAc), 170.2 (NHCO), 167.0 (NP), 164.0 (NP), 156.0 (NP), 150.3 (NP), 147.2 (NP), 132.4 (NP), 125.3 (NP), 116.8 (CF_3), 114.1 (CF_3), 73.2 (Cp), 73.0 (Cp), 72.3 (Cp), 70.7 (Cp), 69.7 (Cp), 68.9 (Cp), 21.4 (Me_{NP}), 17.6 ppm (Me_{NP}); ^{19}F NMR (470 MHz, CD_2Cl_2): δ=−73.8, −74.3, −74.6, −74.7 ppm; IR (KBr): $\tilde{\nu}$=3204 (w; N–H), 3106 (w), 2963 (w), 1678 (s, CO), 1672 (s; CO), 1645 (s; N–H), 1597 (s; OTfAc), 1580 (s; OTfAc), 1514 (s; OTfAc), 1425 (s), 1195 cm^{-1} (vs; CF_3); MS (ESI; CH_3CN): m/z 1314.92 $[M-CF_3COO]^+$; elemental analysis (%) calcd for $C_{50}H_{38}N_6O_{10}F_{12}Fe_2Rh_2$: C 42.04, H 2.68, N 5.88; found: C 42.45, H 2.91, N 5.20.

$[Rh_2(L^2)(L^2H)(CF_3COO)_3]$ (4): Complex **4** was synthesized by following the similar procedure described for the synthesis of complex **3** through a reaction of $Rh_2(CF_3COO)_4$ (50 mg, 0.076 mmol) and L^2H (68 mg, 0.157 mmol) to obtain 78 mg (73%) of product. Red block-shaped crystals of X-ray quality were grown by layering petroleum ether onto a solution of **4** in dichloromethane in a vacuum-sealed glass tube (o.d.=8 mm). ^{1}H NMR (500 MHz, CD_2Cl_2): δ=9.20 (brs, 1H; NH), 7.23–8.46 (br, 18H; NP, Ph), 5.25 (s, 2H; Cp), 5.14 (s, 2H; Cp), 4.74 (s, 2H; Cp), 4.63 (s, 2H; Cp), 4.33 (s, 5H; Cp), 4.27 ppm (s, 5H; Cp); ^{13}C NMR (126 MHz, CD_2Cl_2): δ=175.5 (OTfAc), 173.9 (OTfAc), 171.9 (NHCO), 170.4 (NP), 169.5 (NP), 164.5 (NCO), 163.4 (NP), 156.0 (NP), 154.0 (NP), 149.2 (NP), 147.1 (NP), 141.3 (NP), 140.2 (NP), 134.7 (NP), 131.0 (Ph), 130.1 (Ph), 129.9 (Ph), 129.5, (Ph), 128.8 (NP), 128.0 (NP), 123.0 (NP), 122.4 (NP), 113.3 (CF_3), 111.0 (CF_3), 73.9 (Cp), 73.7 (Cp), 71.4 (Cp), 70.8 ppm (Cp); ^{19}F NMR (470 MHz, CD_3CN): δ=−74.7, −74.8, −74.9, −75.0, −75.2, −75.3, −75.6, −76.2 ppm; IR (KBr): $\tilde{\nu}$=3352 (w; N–H), 3086 (w), 2927 (w), 1675 (s; NHCO), 1642 (s; NCO), 1598 (s; N–H), 1574 (s; OTfAc), 1520 (s; OTfAc), 1477 (s), 1422 (vs), 1198 (vs; CF_3), 1155 cm^{-1} (vs; CF_3); MS (ESI; CH_3CN): m/z 1296.94 $[M-CF_3COO]^+$; elemental analysis (%) calcd for $C_{56}H_{37}N_6O_8F_9Fe_2Rh_2$: C 47.69, H 2.64, N 5.96; found: C 46.78, H 2.98, N 5.42.

$[Rh_2(L^1H)(\mu\text{-}CH_3COO)_2(CH_3CN)_2][(BF_4)_2]$ (5): $[Rh_2(CH_3COO)_2(CH_3CN)_6](BF_4)_2$ (50 mg, 0.067 mmol) was added in one portion to a solution of L^1H (28 mg, 0.074 mmol) in 1,2-dichloroethane (10 mL). The color of the solution became red immediately after this addition. The resulting red solution was heated to reflux for 24 h in a nitrogen atmosphere and cooled to room temperature. The solution was concentrated to a small volume under reduced pressure and diethyl ether (10 mL) was added while stirring to obtain a red precipitate. The precipitate was further washed with diethyl ether (3× 10 mL) and dried under vacuum to afford **5** as a red microcrystalline solid (53 mg, 82%). Block-shaped crystals of X-ray quality were grown by layering petroleum ether onto a solution of **5** in dichloromethane a vacuum-sealed glass tube (o.d.=8 mm). ^{1}H NMR (500 MHz, CD_3CN): δ=9.54 (s, 1H; NH), 8.63 (d, J=8.9 Hz, 1H; NP), 7.76 (d, J=8.9 Hz, 1H; NP),7.62 (s, 1H; NP), 5.35 (s, 1H; Cp), 5.32 (s, 1H; Cp), 4.87 (s, 1H; Cp), 4.86 (s, 1H; Cp), 4.43 (s, 5H; Cp), 3.48 (s, 3H; Me_{NP}), 2.74 (s, 3H; Me_{NP}), 2.42 (s, 3H; Me_{OAc}), 2.13 (s, 6H; CH_3CN), 1.80 ppm (s, 3H; Me_{OAc}); ^{13}C NMR (126 MHz, CD_3CN): δ= 193.4 (CO_{OAc}), 192.1 (CO_{OAc}), 174.6 (NHCO), 172.8 (NP), 163.6 (NP), 157.7 (NP), 153.7 (NP), 152.1 (NP), 140.6 (NP), 127.2 (NP), 122,5 (NP), 78.6 (Cp), 75.3 (Cp), 72.1 (Cp), 70.6 (Cp), 29.5 (Me_{NP}), 24.3 (Me_{OAc}), 22.7 (Me_{OAc}), 18.7 (Me_{NP}), 4.5 (Me_{CH3CN}); IR (KBr): $\tilde{\nu}$=3240 (w; N–H), 3093 (w), 3000 (w), 2938 (w), 2334 (w; CH_3CN), 2306 (w; CH_3CN), 1638 (s, CO), 1592 (m; N–H), 1558 (s; OAc), 1422 (vs), 1063 cm^{-1} (vs; BF_4); MS (ESI; CH_3CN): m/z 877.98 $[M-BF_4]^+$; elemental analysis (%) calcd for $C_{29}H_{31}N_5O_5B_2F_8Fe_1Rh_2$: C 36.10, H 3.24, N 7.26; found: C 35.78, H 2.98, N 7.42.

$[Rh_2(L^2H)_2(\mu\text{-}CH_3COO)_2(CH_3CN)_4][(BF_4)_2]$ (6): $[Rh_2(CH_3COO)_2(CH_3CN)_6](BF_4)_2$ (40 mg, 0.054 mmol) was dissolved in dichloromethane (10 mL) and L^2H (48 mg, 0.111 mmol) was added in one portion. The solution became red immediately and was stirred at room temperature for 30 min. The solution was taken into four glass tubes (o.d.=8 mm), layered with petroleum ether, and sealed under nitrogen. Red block-shaped crystals of **6** were formed after 3—4 days, which were collected and combined for further analysis (36 mg, 44%). ^{1}H NMR (500 MHz, $CDCl_3$): δ=9.06 (brs, 2H; NH), 8.62 (brs, 2H; NP), 8.38 (brs, 2H; NP), 8.26 (brs, 2H; NP), 7.96 (brs, 2H; NP), 7.79 (brs, 4H; Ph), 7.71 (brs, 6H; Ph), 4.52–4.75 (4 s, 8H; Cp), 4.27 (s, 5H; Cp), 4.14 (s, 5H; Cp), 2.25 (s, 3H; Me_{OAc}), 2.16 (s, 3H; Me_{OAc}), 1.97 ppm (brs, 12H; CH_3CN); IR (KBr): $\tilde{\nu}$=3384 (m; N–H), 3352 (m; N–H), 3061 (w), 2980 (w), 2925 (w), 2363 (w; CH_3CN), 2330 (w; CH_3CN), 1676 (s; CO), 1656 (s; N–H), 1567 (s; OAc), 1505 (m), 1452 (vs), 1413 (vs), 1072 cm^{-1} (vs; BF_4); MS (ESI; CH_3CN): m/z 1277.21 $[M-BF_4-CH_3CN)_4]^+$; elemental analysis (%) calcd for $C_{62}H_{56}N_{10}O_6B_2F_8Fe_2Rh_2$: C 48.72, H 3.69, N 9.17; found: C 47.78, H 3.98, N 9.42.

$[Rh_2(L^2H)_2(\mu\text{-}CH_3COO)_2][(BF_4)_2]$ (7): Complex **7** was synthesized by following the similar procedure described for the synthesis of complex **5** by reaction of $[Rh_2(CH_3COO)_2(CH_3CN)_6](BF_4)_2$ (40 mg, 0.054 mmol) and L^2H (48 mg, 0.111 mmol) to obtain 52 mg (71%) of the product. Red block-shaped crystals of X-ray quality were grown by layering diethyl ether onto an solution of **7** in acetonitrile in a vacuum-sealed glass tube (o.d.=8 mm). ^{1}H NMR (400 MHz, CD_3CN): δ=9.35 (s, 1H; NH), 9.34 (s, 1H; NH), 8.95 (s, 2H; NP), 8.39 (d, J=8.2 Hz, 2H; NP), 8.35 (s, 2H; NP), 7.82–7.89 (m, 6H; Ph), 7.71 (d, J=7.8 Hz, 4H; Ph), 7.60 (dd, J=7.8 Hz, 5.5 Hz, 2H; NP), 5.04 (s, 2H; Cp), 4.87 (s, 2H; Cp), 4.76 (s, 2H; Cp), 4.39 (s, 10H; Cp), 4.07 (s, 2H; Cp), 1.96 ppm (s, 6H; Me_{OAc}); ^{13}C NMR (100 MHz, CD_3CN): δ=191.6 (CO_{OAc}), 173.8 (NHCO), 167.8 (NP), 158.9 (NP), 153.1 (NP), 148.5 (NP), 143.5 (NP), 142.8 (NP), 138.9 (NP), 134.4 (NP), 131.7 (Ph), 131.4 (Ph), 130.7 (Ph), 75.7 (Cp), 72.4 (Cp), 71.3 (Cp), 66.2 (Cp), 24.0 ppm (Me_{OAc}); IR (KBr): $\tilde{\nu}$=3363 (m; N–H), 3090 (w), 2926 (w), 1653 (vs; CO), 1597 (s; N–H), 1549 (m), 1518 (s; OAc), 1405 (s), 1083 cm^{-1} (vs; BF_4); MS (ESI; CH_3CN): m/z 1277.21 $[M-BF_4]^+$; elemental analysis (%) calcd for $C_{54}H_{44}N_6O_6B_2F_8Fe_2Rh_2$: C 47.55, H 3.25, N 6.16; found: C 45.98, H 2.96, N 6.22.

General procedure for the catalytic C–H functionalization of indoles

Complex **7** (0.02 mmol, 27 mg) and substituted indole (1 mmol) were dissolved in dry 1,2-dichloroethane (3 mL) in a flame-dried schlenk round-bottomed flask in a nitrogen atmosphere. A solution of ethyl diazoacetate (1.2 mmol, 126 μL) in 1,2-dichloroethane (2 mL) was added dropwise to the resulting solution over 30 min at room temperature. The temperature of the reaction mixture was raised to 60 °C, and the reaction was stirred for 24 h. After completion of the reaction, the solvent was evaporated under reduced pressure and the crude product was purified by flash chromatography on silica gel with ethyl acetate/petroleum ether (2:98) as the

eluent. (For methyl phenyldiazoacetate, complex **7** (14 mg, 0.01 mmol) was taken and the reaction mixture was stirred at room temperature for 12 h. The crude product was purified by flash chromatography on silica gel with ethyl acetate/petroleum ether (5:95) as the eluent.

Acknowledgements

This work was financially supported by the Department of Science and Technology (DST), India. J.K.B. thanks DST for the Swarnajayanti fellowship; M.S. thanks CSIR, India for a fellowship; P.D. thanks CSIR, India for a SPM fellowship; and T.G. thanks UGC India for a fellowship.

Keywords: catalysis · C–H activation · hemilability · hydrogen bonds · naphthyridine · rhodium

[1] a) M. P. Doyle in *Modern Rhodium-Catalyzed Organic Reactions* (Eds.: P. A. Evans), Wiley-VCH, Weinheim, **2005**, pp. 341 – 355; b) D. J. Timmons, M. P. Doyle in *Multiple Bonds Between Metal Atoms* (Eds.: F. A. Cotton, C. A. Murillo, R. A. Walton), Springer, Heidelberg, **2005**, pp. 591 – 632; c) M. P. Doyle, M. A. McKervey, T. Ye, *Modern Catalytic Methods for Organic Synthesis with Diazo Compounds: From Cyclopropanes to Ylides*, Wiley, Hoboken, **1998**; d) H. M. L. Davies, A. R. Dick in *Top. Curr. Chem., Vol. 292* (Eds.: J. Yu, Z. Shi), Springer, Heidelberg, **2010**, pp. 303 – 345; e) K. P. Kornecki, J. F. Berry, D. C. Powers, T. Ritter in *Prog. Inorg. Chem., Vol. 58* (Ed: K. D. Karlin), Wiley, Hoboken, **2014**, pp. 225 – 302; f) M. P. Doyle in *Top. Organomet. Chem., Vol. 13* (Eds.: K. H. Dötz), Springer, Heidelberg, **2004**, pp. 203 – 222 g) K. P. Kornecki, J. F. Briones, V. Boyarskikh, F. Fullilove, J. Autschbach, K. E. Schrote, K. M. Lancaster, H. M. L. Davies, J. F. Berry, *Science* **2013**, *342*, 351 – 354; h) H. M. L. Davies, J. R. Manning, *Nature* **2008**, *451*, 417 – 424.

[2] a) J. Hansen, H. M. L. Davies, *Coord. Chem. Rev.* **2008**, *252*, 545 – 555; b) E. V. Dikarev, D. K. Kumar, A. S. Filatov, A. Anan, Y. Xie, T. Asefa, M. A. Petrukhina, *ChemCatChem* **2010**, *2*, 1461 – 1466; c) D. K. Kumar, A. S. Filatov, M. Napier, J. Sun, E. V. Dikarev, M. A. Petrukhina, *Inorg. Chem.* **2012**, *51*, 4855 – 4861.

[3] a) J. F. Berry, *Dalton Trans.* **2012**, *41*, 700 – 713; b) A. F. Trindade, J. A. S. Coelho, C. A. M. Afonso, L. F. Veiros, P. M. P. Gois, *ACS Catal.* **2012**, *2*, 370 – 383; c) P. Hirva, P. Lahuerta, J. Pe'rez-Prieto, *Theor. Chem. Acc.* **2005**, *113*, 63 – 68; d) J. D. Aguirre, D. A. Lutterman, A. M. Angeles-Boza, K. R. Dunbar, C. Turro, *Inorg. Chem.* **2007**, *46*, 7494 – 7502; e) Y. Lian, K. I. Hardcastle, H. M. L. Davies, *Angew. Chem.* **2011**, *123*, 9542 – 9545; *Angew. Chem. Int. Ed.* **2011**, *50*, 9370 – 9373.

[4] a) P. M. P. Gois, A. F. Trindade, L. F. Veiros, V. André, M. T. Duarte, C. A. M. Afonso, S. Caddick, F. G. N. Cloke, *Angew. Chem.* **2007**, *119*, 5852 – 5855; *Angew. Chem. Int. Ed.* **2007**, *46*, 5750 – 5753; b) A. F. Trindade, P. M. P. Gois, L. F. Veiros, V. Andre', M. T. Duarte, C. A. M. Afonso, S. Caddick, F. G. N. Cloke, *J. Org. Chem.* **2008**, *73*, 4076 – 4086; c) J. A. S. Coelho, A. F. Trindade, R. Wanke, B. G. M. Rocha, L. F. Veiros, P. M. P. Gois, A. J. L. Pombeiro, C. A. M. Afonso, *Eur. J. Org. Chem.* **2013**, 1471 – 1478; d) K. P. Kornecki, J. F. Berry, *Chem. Commun.* **2012**, *48*, 12097 – 12099; e) A. J. Catino, J. M. Nichols, R. E. Forslund, M. P. Doyle, *Org. Lett.* **2005**, *7*, 2787 – 2790; f) A. J. Catino, J. M. Nichols, H. Choi, S. Gottipamula, M. P. Doyle, *Org. Lett.* **2005**, *7*, 5167 – 5170; g) E. C. McLaughlin, M. P. Doyle, *J. Org. Chem.* **2008**, *73*, 4317 – 4319; h) A. J. Catino, R. E. Forslund, M. P. Doyle, *J. Am. Chem. Soc.* **2004**, *126*, 13622 – 13623.

[5] a) Z. Li, H. T. Chifotides, K. R. Dunbar, *Chem. Sci.* **2013**, *4*, 4470 – 4485; b) M. E. Moragues, J. Esteban, J. V. Ros-Lis, R. Martínez-Máñez, M. D. Marcos, M. Martínez, J. Soto, F. Sancenón, *J. Am. Chem. Soc.* **2011**, *133*, 15762 – 15772; c) J. Esteban, J. V. Ros-Lis, R. Martínez-Máñez, M. D. Marcos, M. Moragues, J. Soto, F. Sancenón, *Angew. Chem.* **2010**, *122*, 5054 – 5057; *Angew. Chem. Int. Ed.* **2010**, *49*, 4934 – 4937; d) M. C. Pirrung, A. T. Morehead Jr., *J. Am. Chem. Soc.* **1994**, *116*, 8991 – 9000.

[6] a) J. Lloret, J. J. Carbo', C. Bo, A. Lledós, J. Pérez-Prieto, *Organometallics* **2008**, *27*, 2873 – 2876; b) F. Estevan, P. Lahuerta, J. Pe'rez-Prieto, M. Sanau', S. Stiriba, M. A. Ubeda, *Organometallics* **1997**, *16*, 880 – 886; c) M. P. Doyle, *J. Org. Chem.* **2006**, *71*, 9253 – 9260; d) M. P. Doyle, Q. Zhou, C. E. Raab, G. H. P. Roos, S. H. Simonsen, V. Lynch, *Inorg. Chem.* **1996**, *35*, 6064 – 6073; e) M. P. Doyle, J. P. Morgan, J. C. Fettinger, P. Y. Zavalij, J. T. Colyer, D. J. Timmons, M. D. Carducci, *J. Org. Chem.* **2005**, *70*, 5291 – 5301.

[7] a) F. A. Cotton, E. V. Dikarev, M. A. Petrukhina, *Angew. Chem.* **2000**, *112*, 2452 – 2454; *Angew. Chem. Int. Ed.* **2000**, *39*, 2362 – 2364; b) F. A. Cotton, E. V. Dikarev, M. A. Petrukhina, S. Stiriba, *Organometallics* **2000**, *19*, 1402 – 1405; c) F. A. Cotton, E. V. Dikarev, M. A. Petrukhina, R. E. Taylor, *J. Am. Chem. Soc.* **2001**, *123*, 5831 – 5832; d) F. A. Cotton, E. V. Dikarev, M. A. Petrukhina, *J. Am. Chem. Soc.* **2001**, *123*, 11655 – 11663; e) M. A. Petrukhina, K. W. Andreini, J. Mack, L. T. Scott, *Angew. Chem.* **2003**, *115*, 3497 – 3501; *Angew. Chem. Int. Ed.* **2003**, *42*, 3375 – 3379.

[8] a) T. Oohara, H. Nambu, M. Anada, K. Takeda, S. Hashimoto, *Adv. Synth. Catal.* **2012**, *354*, 2331 – 2338; b) A. Biffis, M. Braga, M. Basato, *Adv. Synth. Catal.* **2004**, *346*, 451 – 458; c) Y. Lou, T. P. Remarchuk, E. J. Corey, *J. Am. Chem. Soc.* **2005**, *127*, 14223 – 14230; d) K. Guthikonda, J. D. Bois, *J. Am. Chem. Soc.* **2002**, *124*, 13672 – 13673; e) A. Padwa, D. J. Austin, A. T. Price, M. A. Semones, M. P. Doyle, M. N. Protopopova, W. R. Winchester, A. Trans, *J. Am. Chem. Soc.* **1993**, *115*, 8669 – 8680; f) M. P. Doyle, M. S. Shanklin, *Organometallics* **1994**, *13*, 1081 – 1088.

[9] a) J. L. Roizen, M. E. Harvey, J. D. Bois, *Acc. Chem. Res.* **2012**, *45*, 911 – 922; b) A. DeAngelis, O. Dmitrenko, G. P. A. Yap, J. M. Fox, *J. Am. Chem. Soc.* **2009**, *131*, 7230 – 7231; c) D. T. Boruta, O. Dmitrenko, G. P. A. Yap, J. M. Fox, *Chem. Sci.* **2012**, *3*, 1589 – 1593; d) A. DeAngelis, D. T. Boruta, J. Lubin, J. N. Plampin, G. P. A. Yap, J. M. Fox, *Chem. Commun.* **2010**, *46*, 4541 – 4543.

[10] a) T. Ren, C. Lin, E. J. Valente, J. D. Zubkowski, *Inorg. Chim. Acta* **2000**, *297*, 283 – 290; b) J. L. Bear, C. L. Yao, R. S. Lifsey, J. D. Korp, K. M. Kadish, *Inorg. Chem.* **1991**, *30*, 336 – 340; c) H. T. Chifotides, K. V. Catalan, K. R. Dunbar, *Inorg. Chem.* **2003**, *42*, 8739 – 8747; d) D. A. Lutterman, N. N. Degtyareva, D. H. Johnston, J. C. Gallucci, J. L. Eglin, C. Turro, *Inorg. Chem.* **2005**, *44*, 5388 – 5396; e) M. W. Cooke, M. P. Santoni, G. S. Hanan, A. Proust, B. Hasenknopf, *Dalton Trans.* **2009**, 3671 – 3673; f) D. Chartrand, G. S. Hanan, *Chem. Commun.* **2008**, 727 – 729.

[11] a) N. G. Connelly, T. Einig, G. G. Herbosa, P. M. Hopkins, C. Mealli, A. G. Orpen, G. M. Rosair, F. Viguri, *J. Chem. Soc. Dalton Trans.* **1994**, 2025 – 2039; b) C. J. Adams, R. A. Baber, N. G. Connelly, P. Harding, O. D. Hayward, M. Kandiah, A. G. Orpen, *Dalton Trans.* **2007**, 1325 – 1333; c) M. B. Hursthouse, M. A. Mazid, T. Clark, S. D. Robinson, *Polyhedron* **1993**, *12*, 563 – 565.

[12] a) F. Estevan, P. Lahuerta, J. Lloret, M. Sanaú, M. A. Ubeda, J. Vila, *Chem. Commun.* **2004**, 2408 – 2409; b) F. Estevan, P. Lahuerta, J. Lloret, J. Pe'rez-Prieto, H. Werner, *Organometallics* **2004**, *23*, 1369 – 1372; c) J. Lloret, F. Estevan, P. Lahuerta, P. Hirva, J. Pe'rez-Prieto, M. Sanaffl, *Chem. Eur. J.* **2009**, *15*, 7706 – 7716; d) F. Estevan, J. Lloret, M. Sanaú, M. A. Úbeda, *Organometallics* **2006**, *25*, 4977 – 4984; e) J. Lloret, M. Stern, F. Estevan, M. Sanaú, M. A. Úbeda, *Organometallics* **2008**, *27*, 850 – 856; f) F. A. Cotton, C. A. Murillo, S. E. Stiriba, X. P. Wang, R. M. Yu, *Inorg. Chem.* **2005**, *44*, 8223 – 8233.

[13] a) M. El-Deftar, F. G. Adly, M. G. Gardiner, A. Ghanem, *Current Organic Chemistry* **2012**, *16*, 1808 – 1836; b) M. P. Doyle, D. C. Forbes, *Chem. Rev.* **1998**, *98*, 911 – 935; c) R. Hrdina, L. Guénée, D. Moraleda, J. Lacour, *Organometallics* **2013**, *32*, 473 – 479; d) C. Qin, V. Boyarskikh, J. H. Hansen, K. I. Hardcastle, D. G. Musaev, H. M. L. Davies, *J. Am. Chem. Soc.* **2011**, *133*, 19198 – 19204; e) R. P. Reddy, G. H. Lee, H. M. L. Davies, *Org. Lett.* **2006**, *8*, 3437 – 3440.

[14] H. M. L. Davies, R. E. J. Beckwith, *Chem. Rev.* **2003**, *103*, 2861 – 2903.

[15] a) W. R. Tikkanen, E. Binamira-Soriaga, W. C. Kaska, P. C. Ford, *Inorg. Chem.* **1983**, *22*, 1147 – 1148; b) W. R. Tikkanen, E. Binamira-Soriaga, W. C. Kaska, P. C. Ford, *Inorg. Chem.* **1984**, *23*, 141 – 146; c) A. T. Baker, W. R. Tikkanen, W. C. Kaska, P. C. Ford, *Inorg. Chem.* **1984**, *23*, 3254 – 3256; d) J. P. Collin, A. Jouaiti, J. P. Sauvage, W. C. Kaska, M. A. McLoughlin, N. L. Keder, W. T. A. Harrison, G. D. Stucky, *Inorg. Chem.* **1990**, *29*, 2238 – 2241; e) A. Sinha, S. M. W. Rahaman, M. Sarkar, B. Saha, P. Daw, J. K. Bera, *Inorg. Chem.* **2009**, *48*, 11114 – 11122; f) S. K. Patra, N. Sadhukhan, J. K. Bera, *Inorg. Chem.* **2006**, *45*, 4007 – 4015; g) M. Majumdar, S. K. Patra, M. Kannan, K. R. Dunbar, J. K. Bera, *Inorg. Chem.* **2008**, *47*, 2212 – 2222; h) C. S. Campos-Fernández, X. Ouyang, K. R. Dunbar, *Inorg. Chem.* **2000**,

39, 2432 – 2433; i) C. S. Campos-Fernández, L. M. Thomson, J. R. Galán-Mascarós, X. Ouyang, K. R. Dunbar, *Inorg. Chem.* **2002**, *41*, 1523 – 1533.
[16] a) V. P. Litvinov, *Adv. Heterocycl. Chem.* **2006**, *91*, 189 – 300; b) C. He, S. J. Lippard, *Tetrahedron* **2000**, *56*, 8245 – 8252; c) J. Kuzelka, S. Mukhopadhyay, B. Spingler, S. J. Lippard, *Inorg. Chem.* **2003**, *42*, 6447 – 6457; d) C. He, S. J. Lippard, *Inorg. Chem.* **2001**, *40*, 1414 – 1420; e) T. C. Davenport, T. D. Tilley, *Angew. Chem.* **2011**, *123*, 12413 – 12416; *Angew. Chem. Int. Ed.* **2011**, *50*, 12205 – 12208.
[17] R. K. Das, B. Saha, S. M. W. Rahaman, J. K. Bera, *Chem. Eur. J.* **2010**, *16*, 14459 – 14468.
[18] N. Sadhukhan, A. Sinha, R. K. Das, J. K. Bera, *J. Organomet. Chem.* **2010**, *695*, 67 – 73.
[19] a) A. Sinha, M. Majumdar, M. Sarkar, T. Ghatak, J. K. Bera, *Organometallics* **2013**, *32*, 340 – 349; b) M. Brookhart, M. L. H. Green, G. Parkin, *Proc. Nat. Acad. Sci. USA* **2007**, *104*, 6908 – 6914.
[20] H. Kitamura, T. Ozawa, K. Jitsukawa, H. Masuda, Y. Aoyama, H. Einaga, *Inorg. Chem.* **2000**, *39*, 3294 – 3300.
[21] J. D. Carr, S. J. Coles, W. W. Hassan, M. B. Hursthouse, K. M. Abdul Malik, J. H. R. Tucker, *J. Chem. Soc. Dalton Trans.* **1999**, 57 – 62.
[22] F. A. Cotton, E. A. Hillard, C. A. Murillo, *J. Am. Chem. Soc.* **2002**, *124*, 5658 – 5660.
[23] F. A. Cotton, K. R. Dunbar, M. G. Verbruggen, *J. Am. Chem. Soc.* **1987**, *109*, 5498 – 5506.
[24] C. A. Crawford, J. H. Matonic, J. C. Huffman, K. Folting, K. R. Dunbar, G. Christou, *Inorg. Chem.* **1997**, *36*, 2361 – 2371.
[25] a) M. P. Doyle, R. Duffy, M. Ratnikov, L. Zhou, *Chem. Rev.* **2010**, *110*, 704 – 724; b) H. M. L. Davies, D. Morton, *Chem. Soc. Rev.* **2011**, *40*, 1857 – 1869; c) C. N. Slattery, A. Ford, A. R. Maguire, *Tetrahedron* **2010**, *66*, 6681 – 6705.
[26] a) P. M. Dewick, *Medicinal Natural Products: A Biosynthetic Approach*, Wiley, Hoboken, **2009**; b) D. H. R. Barton, K. Nakanishi, O. MethCohn, J. W. Kelly, *Comprehensive Natural Products Chemistry*, Pergamon Press, Oxford, **1999**; c) A. J. Kochanowska-Karamyan, M. T. Hamann, *Chem. Rev.* **2010**, *110*, 4489 – 4497.
[27] H. M. L. Davies, S. J. Hedley, *Chem. Soc. Rev.* **2007**, *36*, 1109 – 1119.
[28] E. Wenkert, M. E. Alonso, H. E. Gottlieb, E. L. Sanchez, R. Pellicciari, P. Cogolli, *J. Org. Chem.* **1977**, *42*, 3945 – 3949.
[29] J. M. Fraile, K. L. Jeune, J. A. Mayoral, N. Ravasiob, F. Zaccheria, *Org. Biomol. Chem.* **2013**, *11*, 4327 – 4332.
[30] S. J. Hedley, D. L. Ventura, P. M. Dominiak, C. L. Nygren, H. M. L. Davies, *J. Org. Chem.* **2006**, *71*, 5349 – 5356.
[31] S. Muthusamy, C. Gunanathan, S. Arulananda Babu, E. Suresh, P. Dastidar, *Chem. Commun.* **2002**, 824 – 825.
[32] A. DeAngelis, V. W. Shurtleff, O. Dmitrenko, J. M. Fox, *J. Am. Chem. Soc.* **2011**, *133*, 1650 – 1653.
[33] Y. Lian, H. M. L. Davies, *Org. Lett.* **2012**, *14*, 1934 – 1937.
[34] M. B. Johansen, M. A. Kerr, *Org. Lett.* **2010**, *12*, 4956 – 4959.
[35] W. Chan, S. Yeung, Z. Zhou, A. S. C. Chan, W. Yu, *Org. Lett.* **2010**, *12*, 604 – 607.
[36] Y. Cai, S. Zhu, G. Wang, Q. Zhou, *Adv. Synth. Catal.* **2011**, *353*, 2939 – 2944.
[37] R. Gibe, M. A. Kerr, *J. Org. Chem.* **2002**, *67*, 6247 – 6249.
[38] E. Nakamura, N. Yoshikai, M. Yamanaka, *J. Am. Chem. Soc.* **2002**, *124*, 7181 – 7192.
[39] M. Sarkar, J. K. Bera, *Proc. Natl. Acad. Sci. India, Sect. A* **2014**, *84*, 227 – 234.
[40] G. A. Rempel, P. Legzdins, H. Smith, G. Wilkinson in *Inorganic Syntheses, Vol. 13* (Ed.: F. A. Cotton), McGraw-Hill, New York, **1972**, pp. 90 – 91.
[41] G. Pimblett, C. D. Garner, W. Clegg, *J. Chem. Soc. Dalton Trans.* **1986**, 1257 – 1263.

Received: April 3, 2014
Published online on October 21, 2014